

Methods.....	1
Supplementary Figure DR1 – Previous UHP Data from Tso Morari.....	2
Supplementary Figure DR2 – Representative Analyses Map.....	3
Supplementary Figure DR3 – Cathodoluminescence Images.....	4
Supplementary Figure DR4 – Intercept and ²⁰⁷Pb-corrected Ages by Texture	5
Supplementary Figure DR5 – Garnet profiles and X-Ray Maps	6
Supplementary Table DR1 – LA-ICP-MS Split Stream U-Th-Pb Analyses	7
Supplementary Table DR2 – LA-ICP-MS Split Stream Rare Earth Element Analyses	8
Supplementary Table DR3 – Timing of Collision Calculation Table	9

Methods

U–Pb zircon petrochronology was performed at the University of California, Santa Barbara LASS lab (<http://sites.google.com/site/icpgeolucsb/>) using a Nu Plasma HR MC-ICPMS, a Nu AttoM SC-ICPMS (Nu Instruments Ltd., Wrexham, UK) and an Analyte 193 excimer ArF laser-ablation system equipped with a HeLex sample cell (Photon Machines, San Diego, USA). The analytical setup is described in Table 1. The ablated aerosol is carried by He from the sample cell to a mixing bulb in which the sample + He is mixed with Ar to stabilize the aerosol input to the plasma. The He-Ar-aerosol is immediately split upon exiting the mixing bulb, with approximately half the ablation stream directed to each ICPMS. Laser energy is set to 4 mJ, which, once transmitted into the sample chamber, equates to $\sim 0.1 \mu\text{m}/\text{pulse}$; repetition rate is set to 4 Hz; single-ablation duration was 20–25 seconds; and spot diameters ranged from 12–14 μm with depths of $\sim 8 \mu\text{m}$.

U–Pb dates were obtained with the Nu Plasma, equipped with four low-mass side electron multipliers for simultaneous measurement of ^{208}Pb , ^{207}Pb , ^{206}Pb and ^{204}Pb ; ^{238}U and ^{232}Th were measured on Faraday cups equipped with 1011-ohm resistors. The Nu AttoM was used in "E-Scan" mode to measure REE and Hf concentrations. Because standard analyses are matrix-matched (see below), internal standardization was unnecessary. Sample analyses were preceded by a 10-second baseline measurement, and unknown analyses were corrected with the 91500 zircon standard (Wiedenbeck et al. 1995) every 7 measurements (~ 5 min.). For quality control, the zircon reference material GJ1 (601 Ma, Jackson et al., 2004) was run after each 91500 analysis, and yielded a

$^{206}\text{Pb}/^{238}\text{U}$ age of 609.8 ± 2.5 Ma ($n = 34$; MSWD = 1.5; in-run error). The Plešovice reference material (Slama et al., 2008) was also analyzed throughout the analytical session and yielded a concordia age of 337.6 ± 0.9 Ma ($n = 27$; MSWD = 0.76; in-run error). Post-data processing was performed using Iolite (Paton et al., 2010), and concordia plots were produced with Isoplot (Ludwig, 2003).

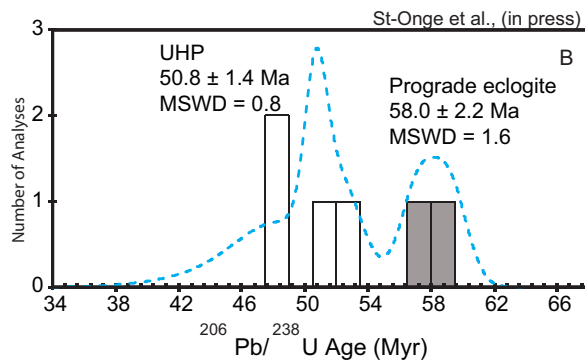
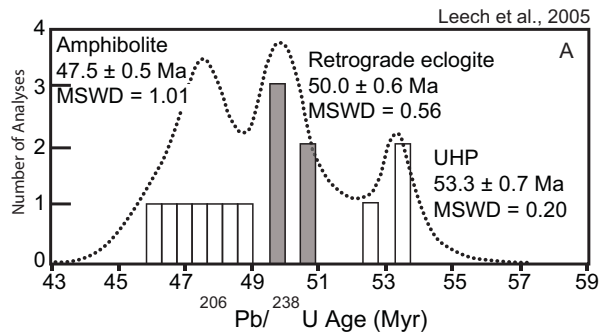
Supplementary Figure DR1 Probability Density Function of $^{238}\text{U}/^{206}\text{Pb}$ ages (^{207}Pb -corrected) from Leech et al. (2005) and St-Onge et al. (in press). Displayed ages represent Concordia intercept ages of subpopulations as provided by the original authors; age significance is also as proposed by the original authors.

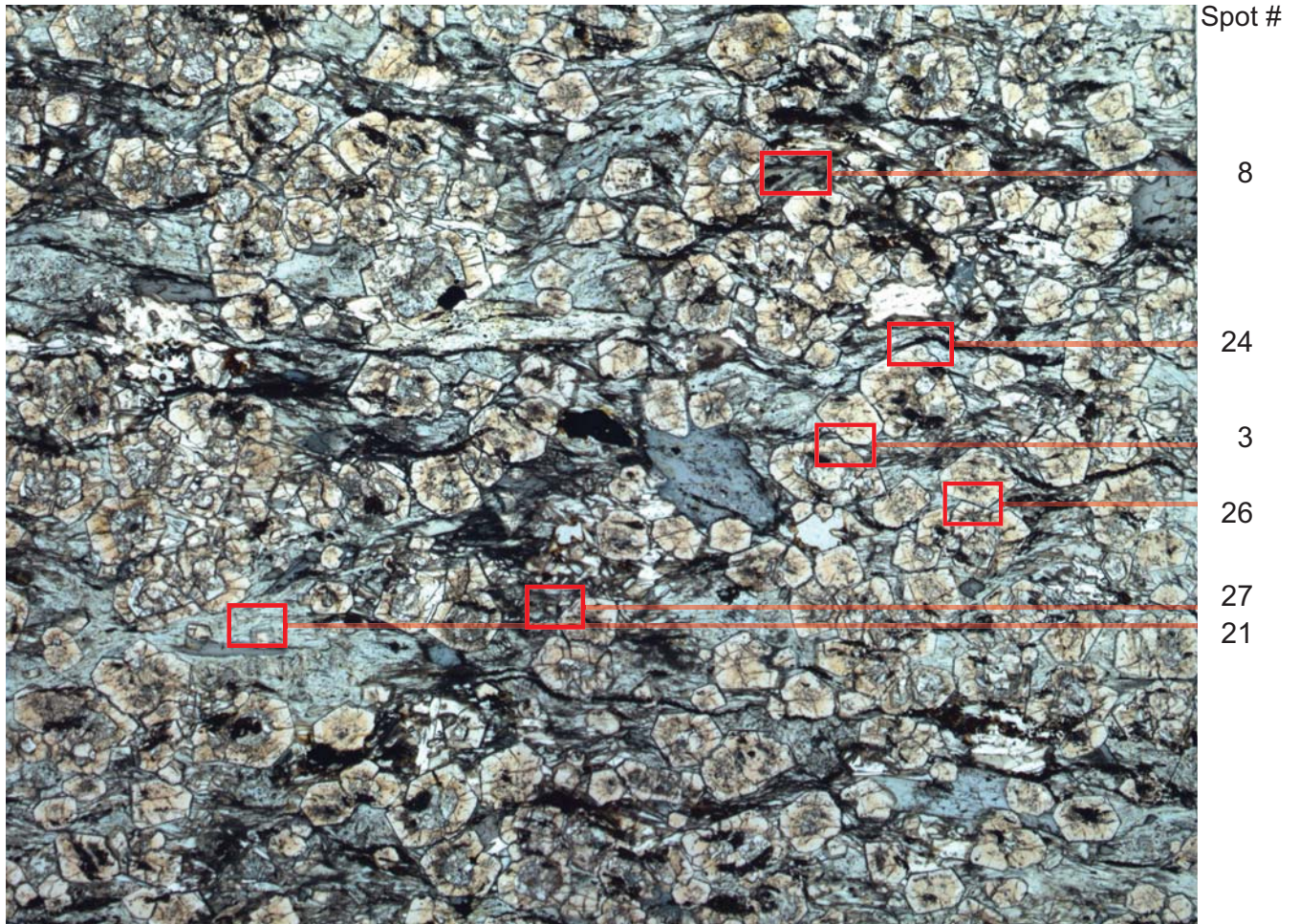
Zircon geochronology data sets of Leech et al. (2005) and St-Onge et al. (in press) do not provide sufficient information to resolve the timing of peak (UHP) metamorphism (cf. Fig. 3).

There are two challenges with the Leech et al. (2005) data set: 1) There is no petrologic evidence to associate zircon growth with metamorphic events. This is because the analyses were not in situ and information about inclusions within zircon grain separates was not presented. 2) The data are not as statistically meaningful as those authors suggest. For instance, the mean square weighted deviates (MSWD) statistic is provided, but this statistic only begins to provide meaningful resolution of an age population when the number of analyses is at least 5 (Wendt and Carl, 1991). The resolution for discerning multiple age populations increases as the number of analyses increases. All of the interpreted ages for HP/UHP events by Leech et al. (2005) are based on a small number of analyses (n=5,3 respectively).

St-Onge et al. (in press) provide petrologic information defining Tso Moriri eclogitic assemblages in relation to dated zircon. These authors analyzed spots from zircon included in garnet cores, which yielded the interpreted prograde age; and matrix zircon spots, which yielded the interpreted peak (UHP) age. The matrix zircons are in association with phengite, rutile, barroisite and omphacite (one of the analyzed 'matrix' zircons is included in omphacite). The dated matrix zircons have similar Th/U ratios, morphology, and zonation patterns to an undated zircon included in UHP garnet, and are thus interpreted by St-Onge et al. to have crystallized at UHP conditions.

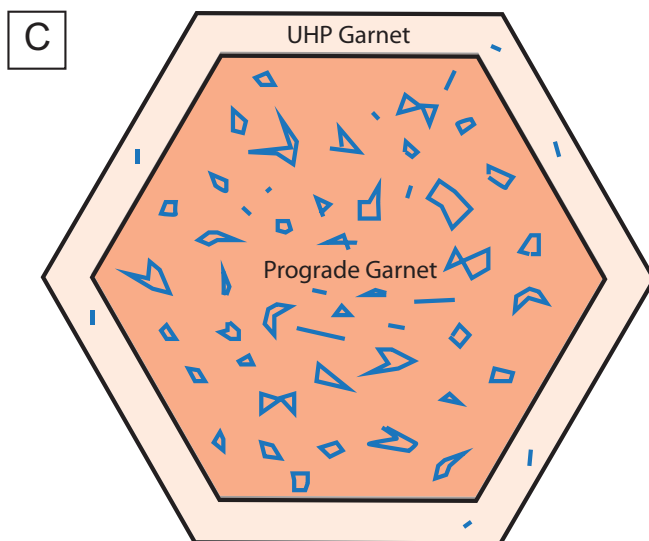
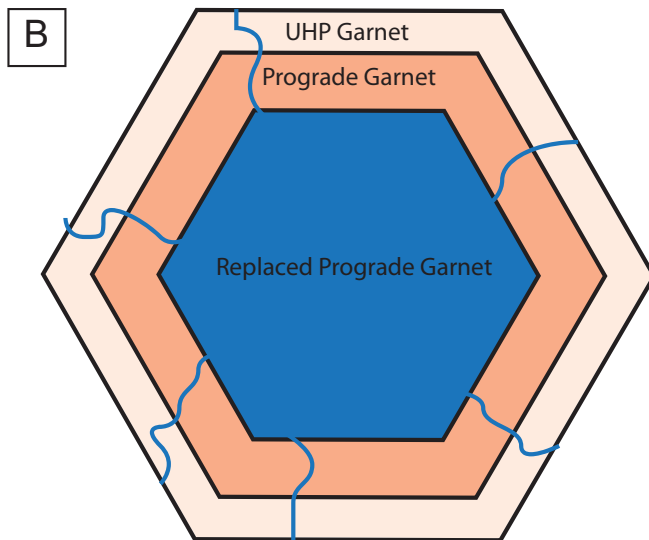
St-Onge et al. (in press) did not resolve the second challenge of an insufficient number of analyses. St-Onge et al. (in press) analyzed two zircons included in garnet cores (prograde, eclogitic) and only four zircons interpreted to crystallize at UHP conditions. Three of the four UHP age results are highly discordant, such that the interpreted UHP U-Pb intercept age is dominantly determined by projection through just one nearly concordant zircon analysis (see their Figure 17).





Supplementary Figure DR2 A . Representative image of CM71710-4 petrographic thin section. Boxes represent area of analyses denoted with the number corresponding to Figure A3 and Table A1.

In the following sections of Figure A2 representative transmitted, cross polarized and reflected light images of the analyzed zircon. The images demonstrate the major zircon settings: 1) Zircons included in UHP garnet. 2) Zircons included in omphacite. 3) Zircons in the matrix. Example of garnet structures can be found in A3-B and A3-C.



Supplementary Figure DR2. Illustration showing the garnet characteristics in both samples. Detailed descriptions of UHP Tso Morari garnets can be found in O'Brien, 2006 and Konrad-Schmolke et al., 2008. B) Atoll garnet structure, "Replaced Prograde Garnet" was previous Ca-rich garnet that has been consumed and replaced by other HP-UHP minerals. This zone is also referred to as the core of the atoll garnet. "Prograde Garnet", is the Ca-rich remnants that have survived consumption at HP and UHP metamorphism. "UHP Garnet" is the Mg-rich overgrowth in which coesite is typically found in UHP eclogites indicating growth at UHP conditions. C) Garnet with Ca-rich high inclusion idioblastic core and Mg-rich low inclusion rim. "Prograde Garnet" is the idioblastic Ca-rich core. "UHP Garnet" is the Mg-rich rim.

Supplementary Figure DR2 (Spot 3)

Zircon in UHP garnet

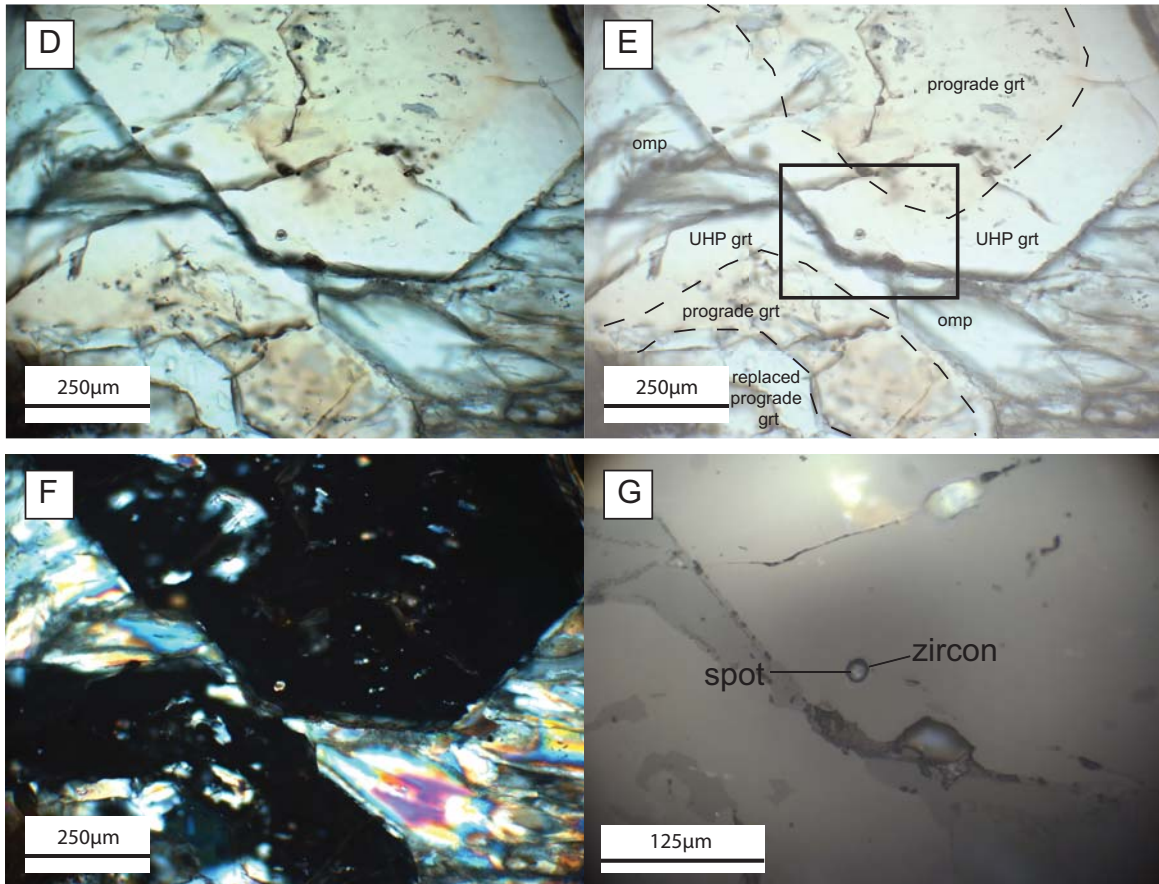


Figure DR2 (Spot 3): D is a TL image of the sample; E is an annotated version of D; F is XPL image; G is a reflected light image. grt = garnet; omp= omphacite; Spot signals where zircon was shot.

Supplementary Figure DR2 (Spot 26)

Zircon in UHP garnet

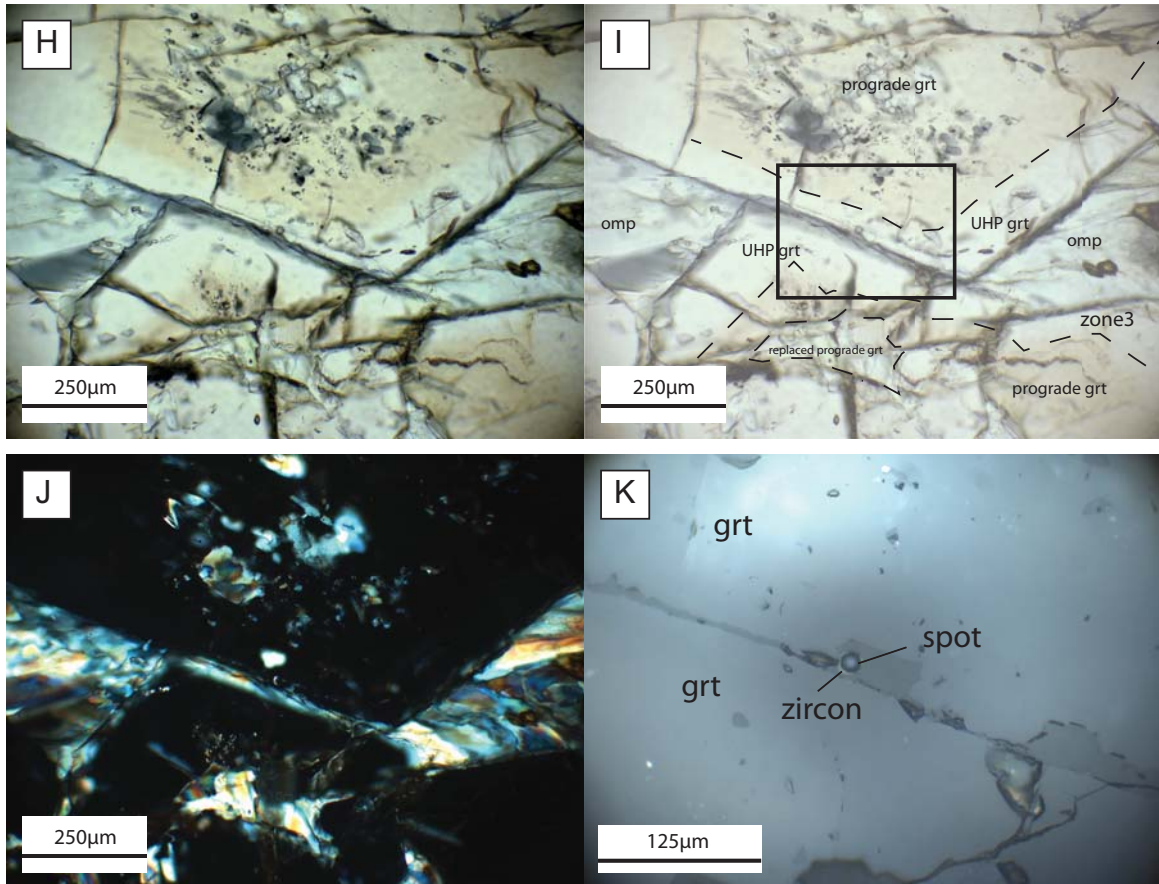


Figure DR2 (Spot 26) H is a TL image of the sample; I is an annotated version of H.; J is XPL image; K is a reflected light image; grt = garnet; omp= omphacite; Spot signals where zircon was shot.

Supplementary Figure DR2 (Spot 21)

Zircon in omphacite

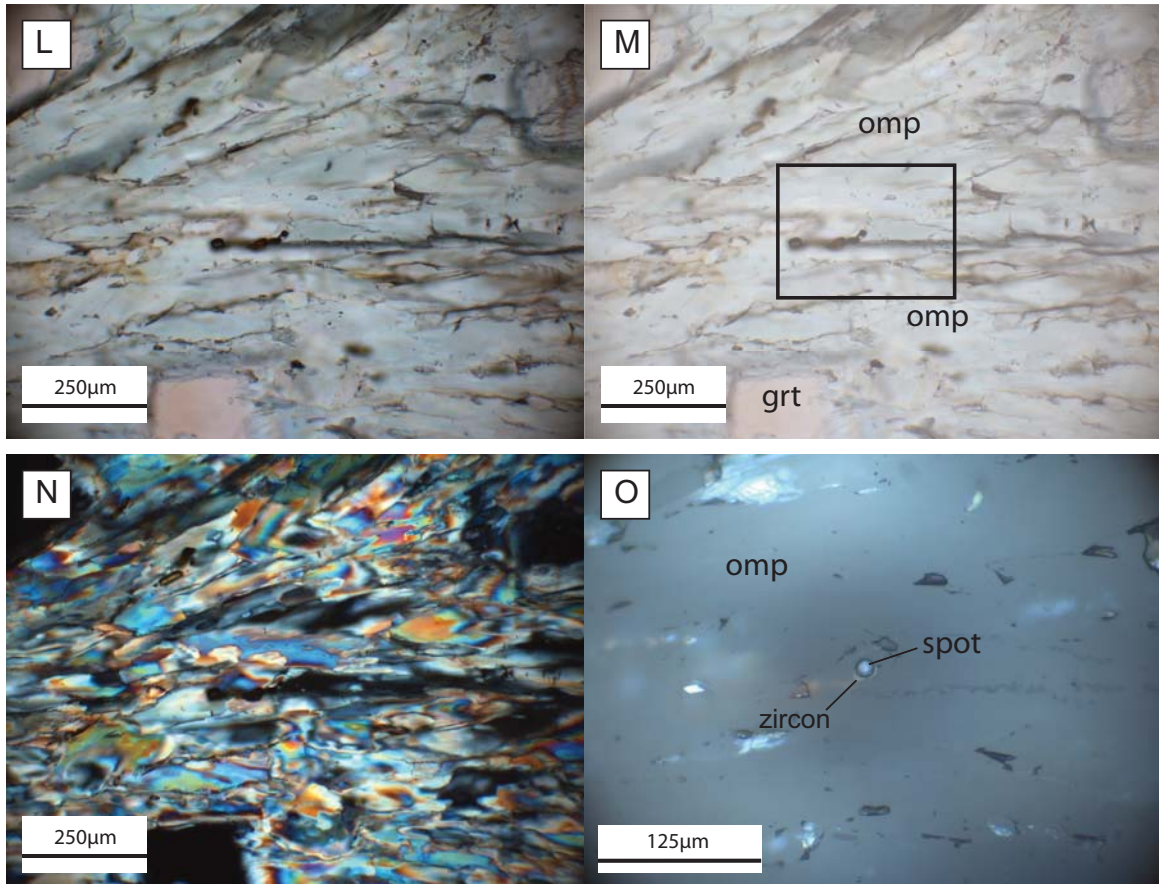


Figure DR2 (Spot 21), L is a TL image of the sample; M is an annotated version of L; N is XPL image; M is a reflected light image; grt = garnet; omp= omphacite; rut = rutile. Spot signals where zircon was shot.

Supplementary Figure DR2 (Spot 27)

Zircon in omphacite

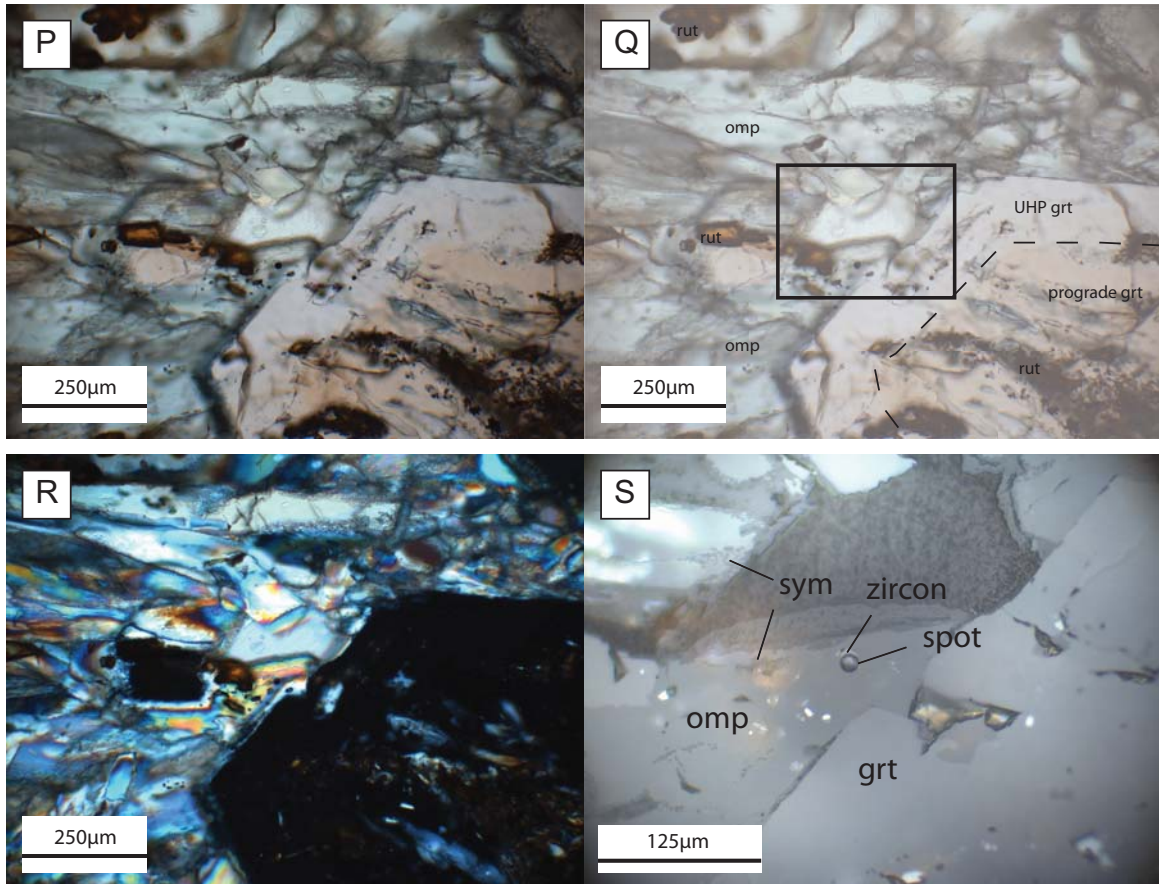


Figure DR2 (Spot 27), P is a TL image of the sample; Q is an annotated version of P; R is XPL image; S is a reflected light image; grt = garnet; omp= omphacite; sym = symplectite rut = rutile. Spot signals where zircon was shot.

Supplementary Figure DR2 (Spot 8)

Zircon in matrix

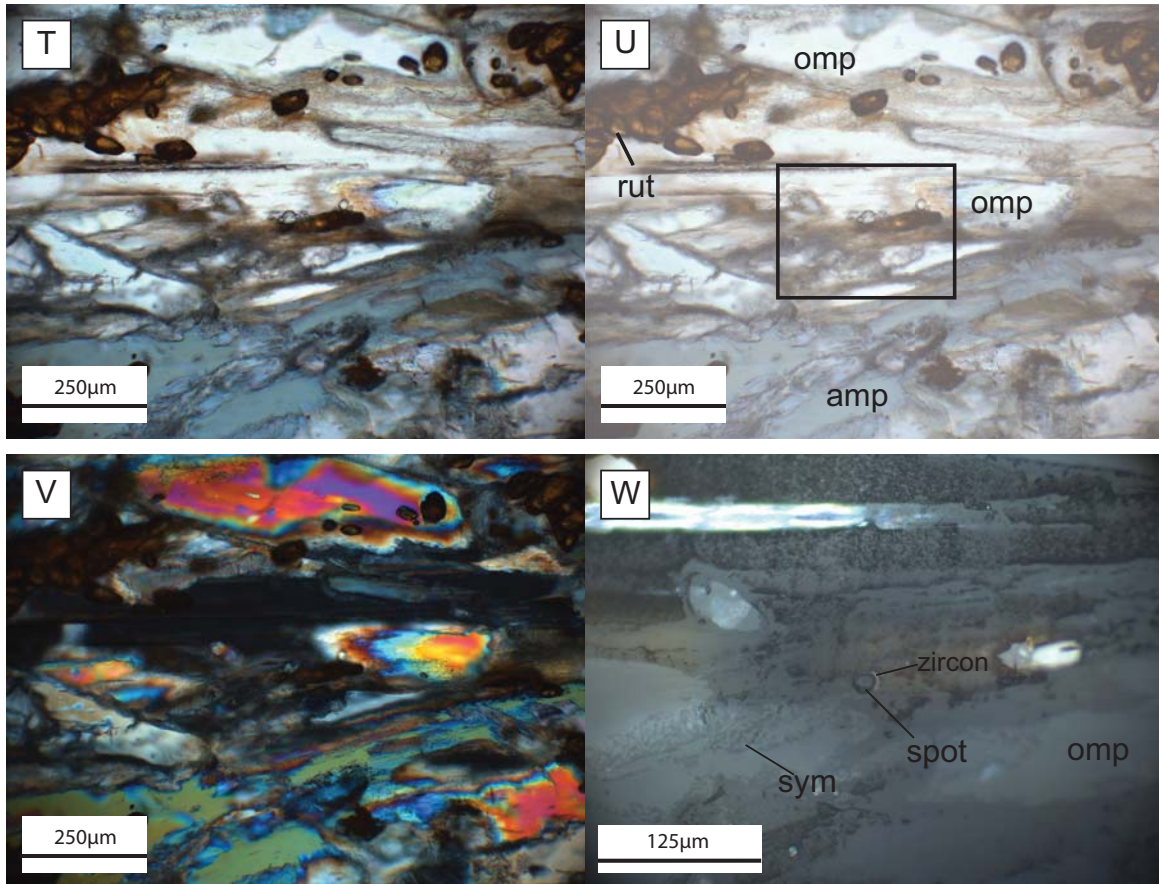


Figure DR2 (Spot 8), T is a TL image of the sample; U is an annotated version of T; V is XPL image; W is a reflected light image. amp = amphibole; omp= omphacite; sym = symplectite rut = rutile. Spot signals where zircon was shot.

Supplementary Figure DR2 (Spot 24)

Zircon in the matrix

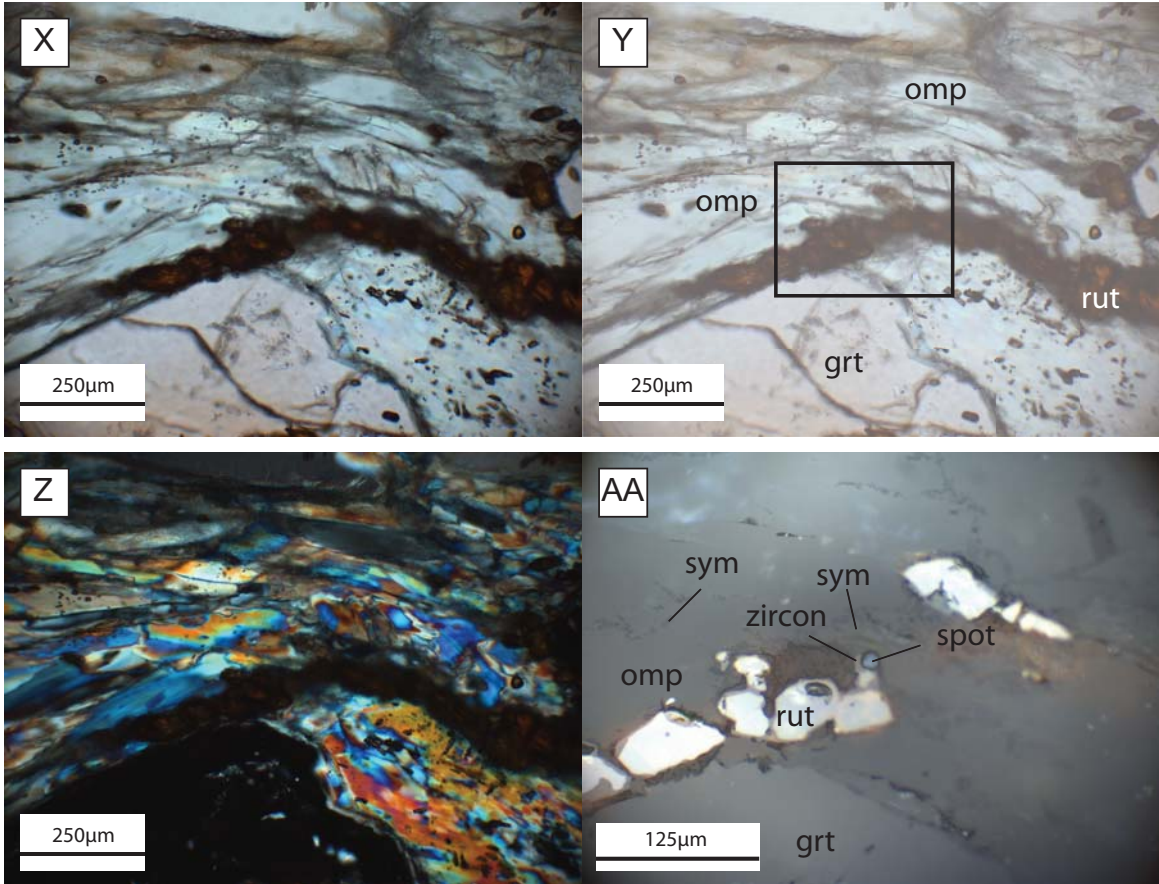
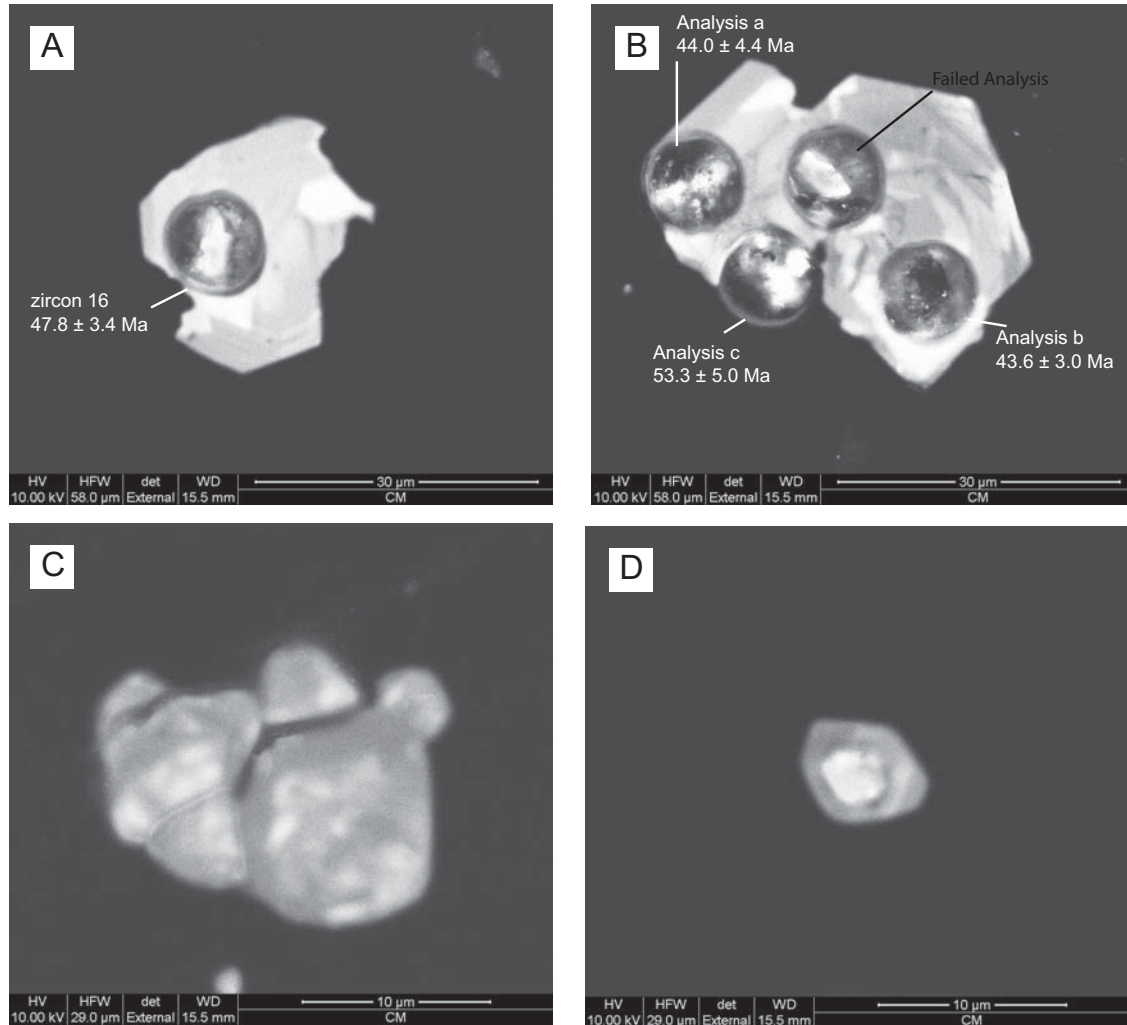


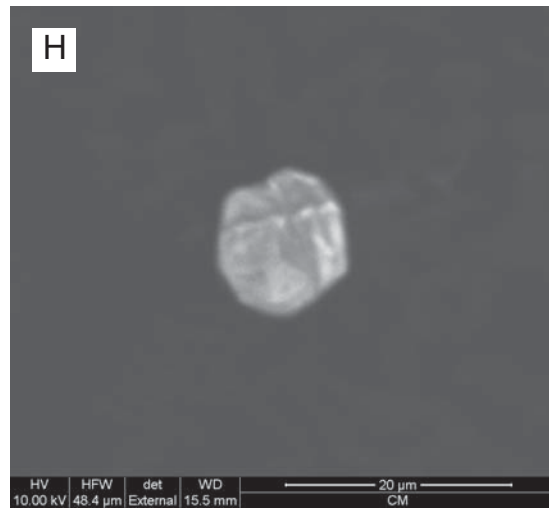
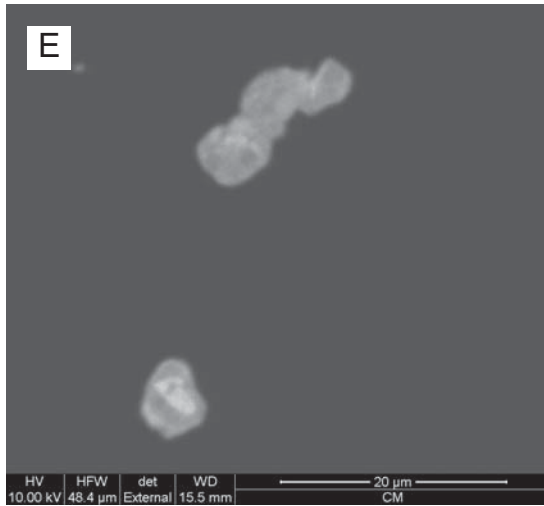
Figure DR2 (Spot 24), X is a TL image of the sample; Y is an annotated version of X; Z is XPL image; AA is a reflected light image; grt = garnet; omp= omphacite; sym = symplectite; rut = rutile. Spot signals where zircon was shot.

Supplementary Figure DR3 Cathodoluminescence images of *in situ* zircon grains from CM71710-4 and DD71710-2b eclogites. Images show zoning characteristics of analysed and representative zircons. Cathodoluminescence of zircon can reveal the internal structure of the mineral and distinguish between homogenous and heterogenous crystallization. The majority of the images exhibit irregular patchy zoning similar to “auroral lights” zoning (Corfu et al., 2003) indicative of a high pressure event. Images A-B of A3 are of analyzed spots which generally show oscillatory zoning with possibility of recrystallization indicative of brighter illumination regions in the grain. Images with defined cores can be interpreted to have older and younger generations of growth. Unclear zoning of some images may result from unpolished zircon surface of *in situ* grains.

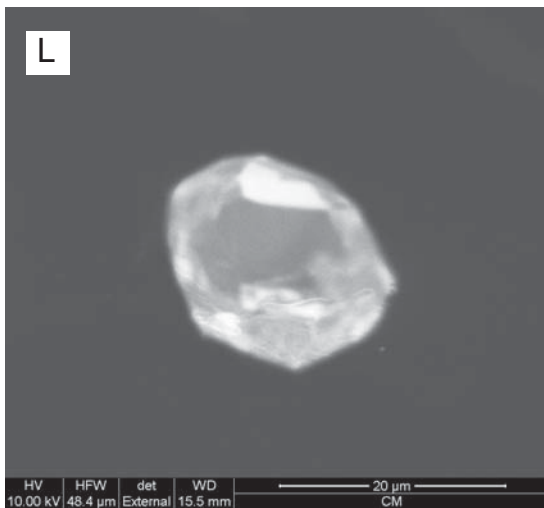
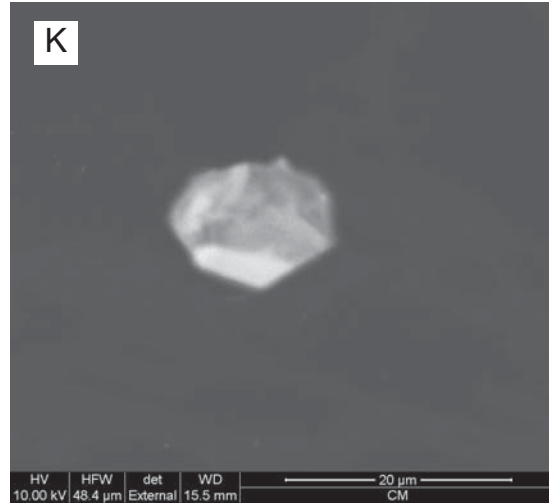
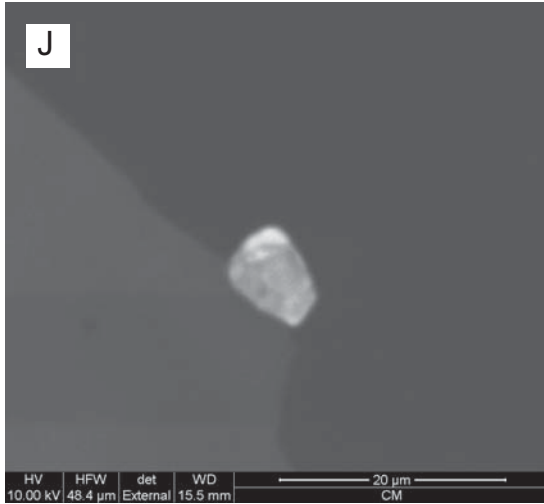


Supplementary Figure DR3 - Cathodoluminescence Images in CM71710-4 A)

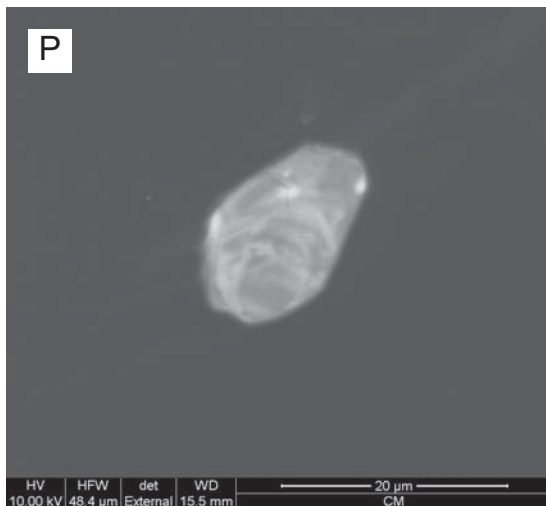
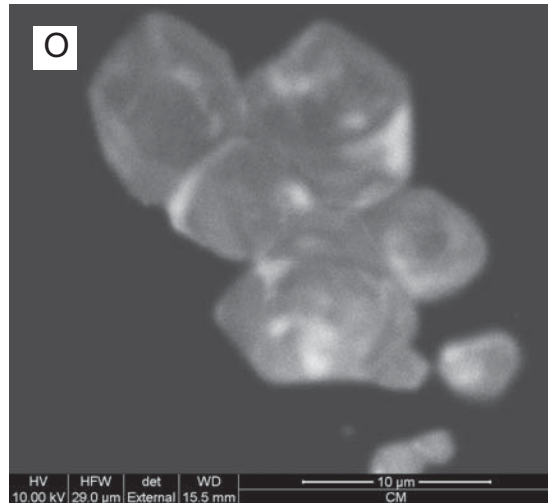
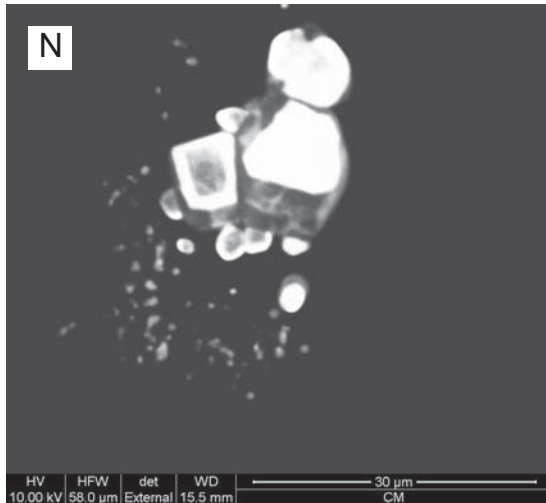
CL image of zircon shot in analysis 16 = 47.8 ± 3.4 Ma . Image shows possible recrystallization in brighter areas outside of spot diameter. Zoning is generally oscillatory. B) CL image of zircon shot in analyses 31a-c. Fourth image analysis in the center of the image was not within detection limits of the rest of the analyses. “Analysis a” has a 207-Pb-corrected age of 44.0 ± 4.4 Ma; “Analysis b” = 43.6 ± 3.0 Ma; “Analysis c” 53.3 ± 5.0 Ma. Zoning appears to be heterogeneously patchy. C) CL image of zircon cluster included in UHP garnet rim. Zoning is irregular and patchy . D)CL image of zircon grain included in UHP garnet. Zoning appears heterogeneous with a distinct core and metamorphic rim.



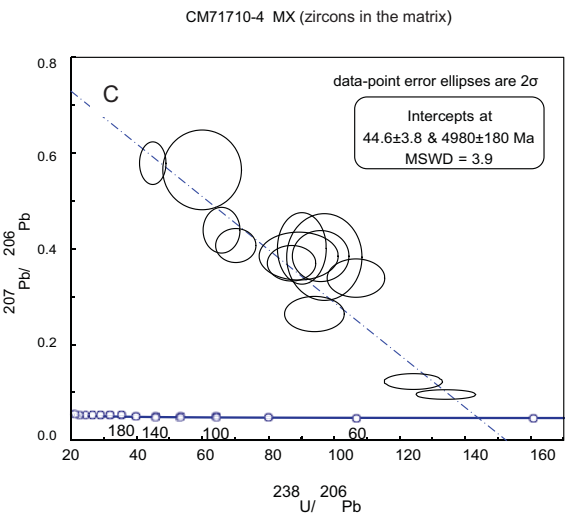
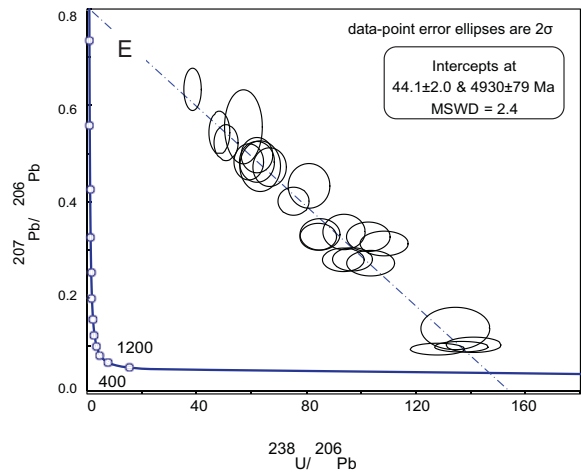
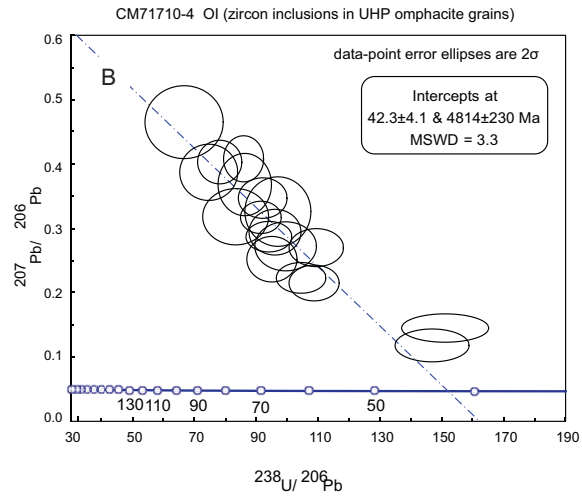
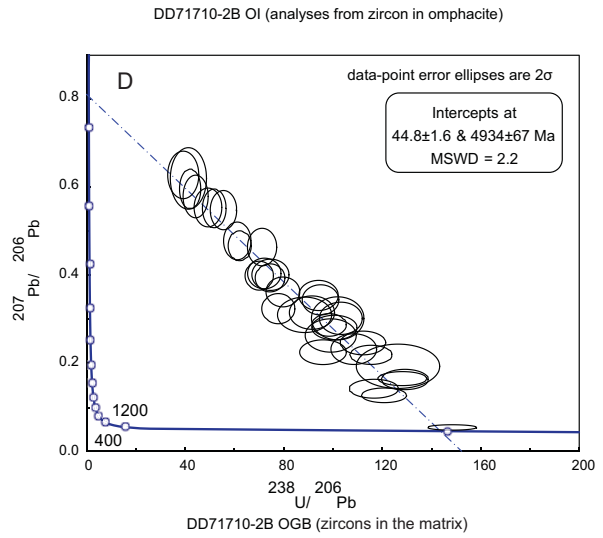
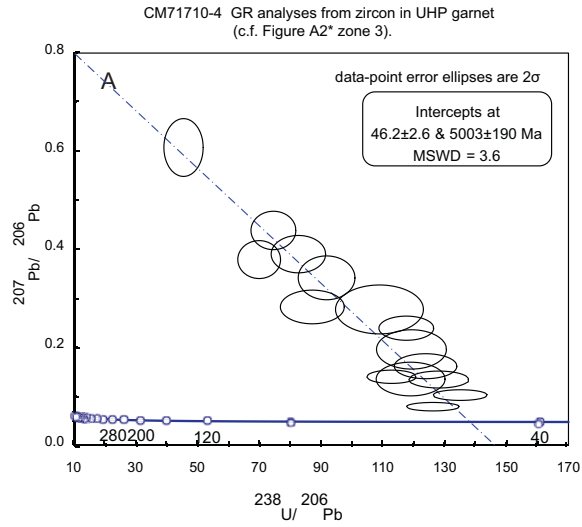
Supplementary Figure DR3 continued - Cathodoluminescence Images in DD71710-2b. E) CL image of zircon cluster included in UHP garnet. Zoning is irregular patchy. Lone zircon appears to have a distinct core. F) CL image of zircon in the matrix with irregular and patchy zoning. G) CL image of zircon in matrix near symplectite. Zoning is irregularly patchy with possible metamictization. H) CL image of zircon in the matrix near symplectite. Zoning is irregularly patchy with possible metamictization.



Supplementary Figure DR3 continued - Cathodoluminescence Images in DD71710-2b. J) CL of a zircon in the matrix near garnet/omphacite grain boundary with irregular patchy zoning. K) CL of zircon near a rutile grain in matrix. Zoning is generally patchy besides the lower end of the grain which exhibits higher contrast. L) CL of zircon in the matrix. The grain exhibits a core and a possible zone of recrystallization, indicative of the higher contrast region at the top of the grain.

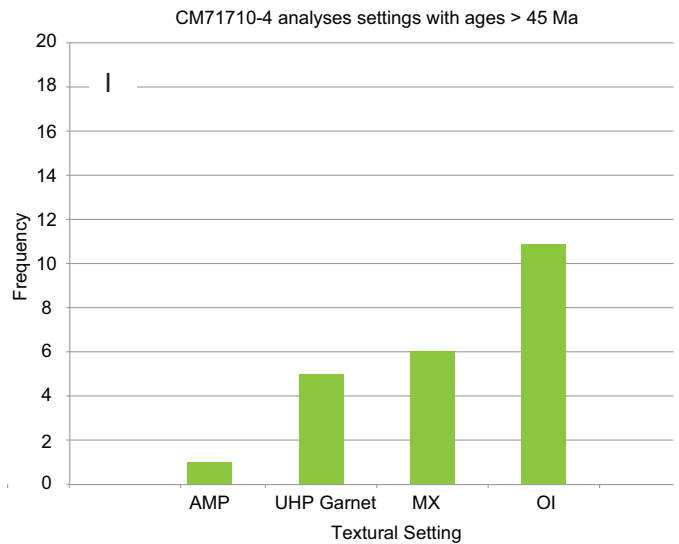
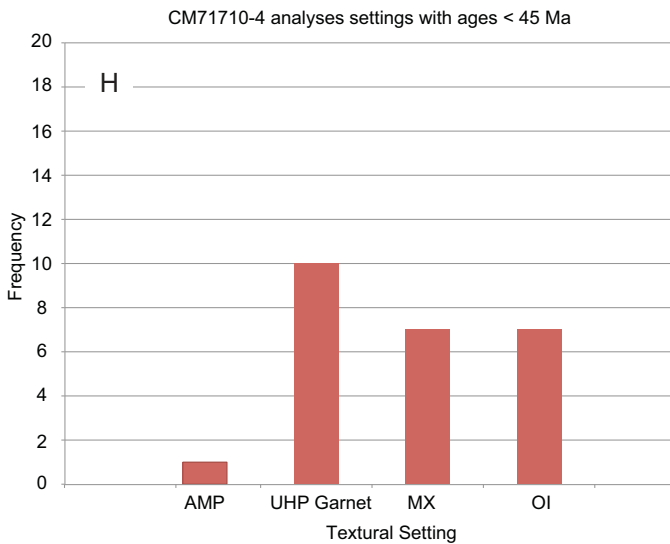
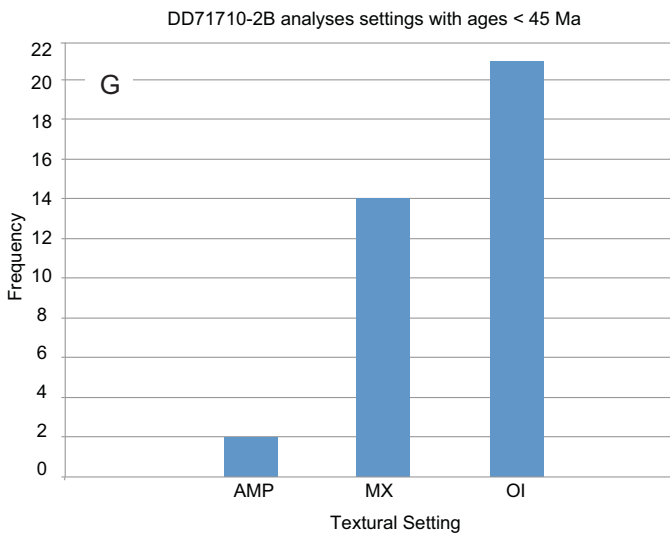
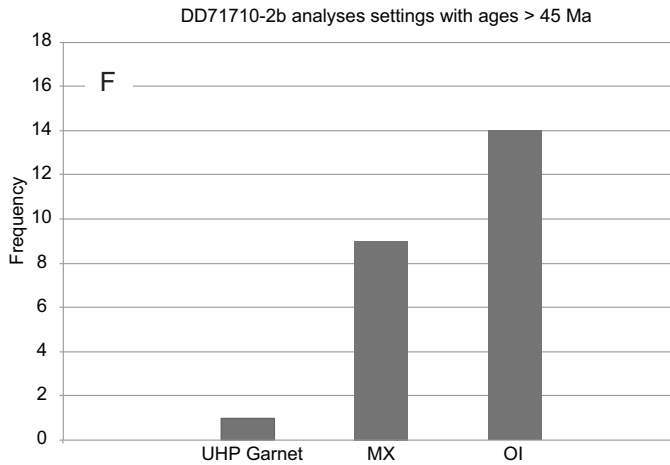


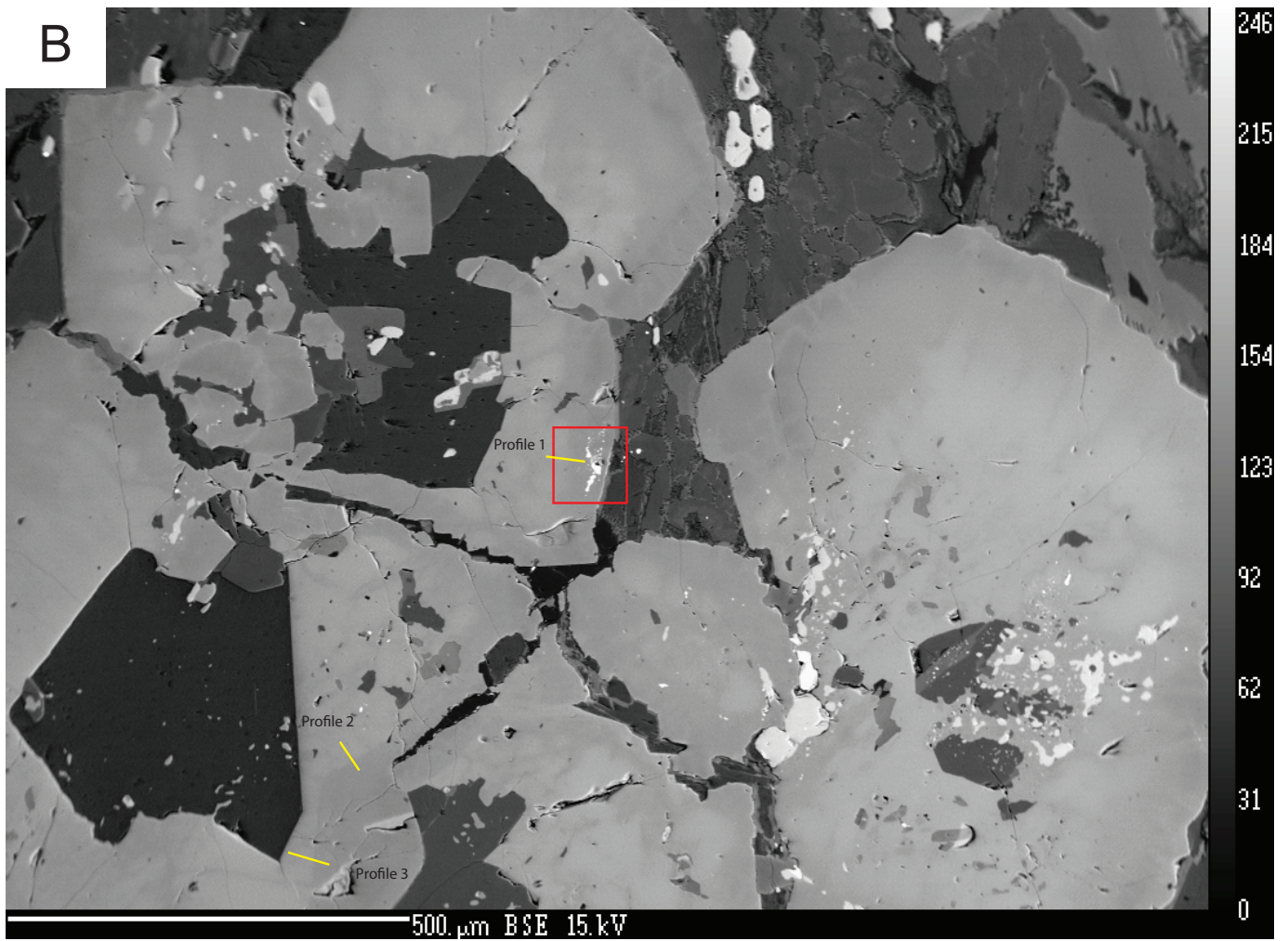
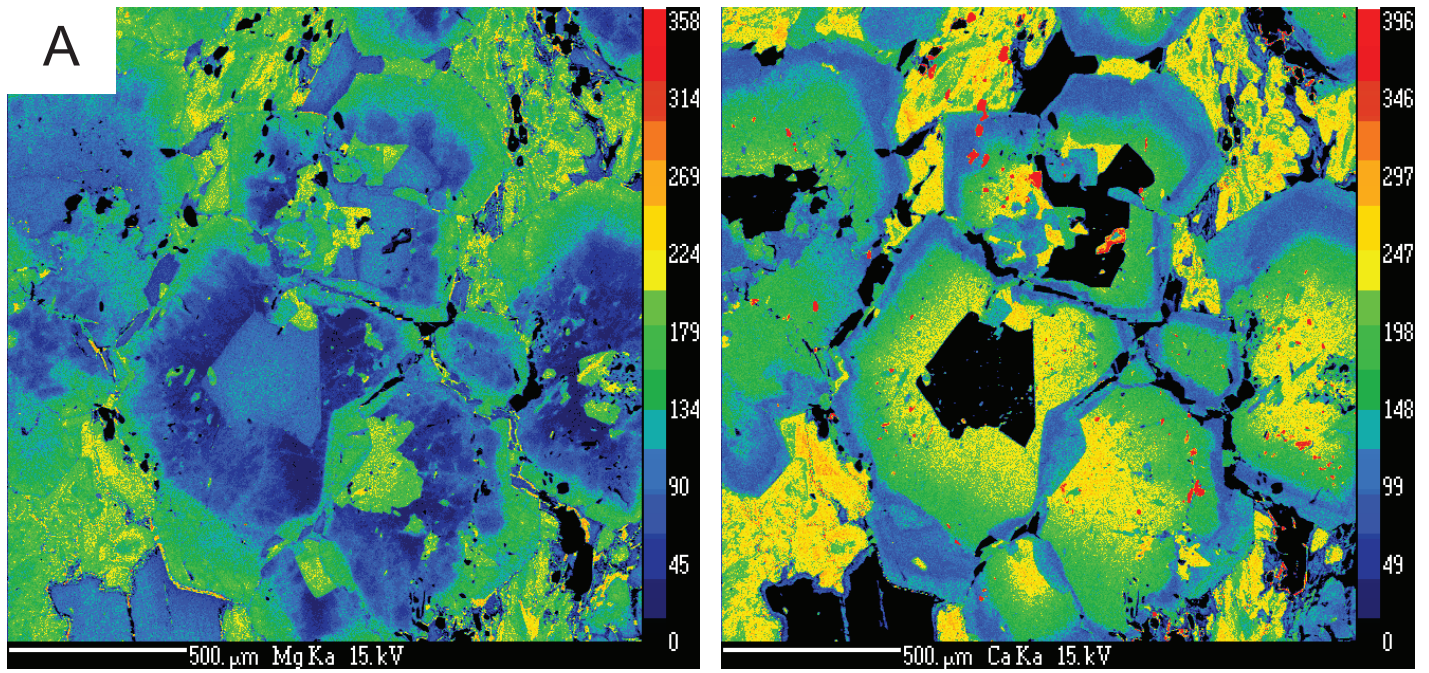
Supplementary Figure DR3 Cathodoluminescence Images in CM71710-4 (M-O) and DD71710-2b (P). N) CL image of zircon cluster in the matrix with defined areas of metamorphic rim growth indicative of the darker contrast. O) CL image of zircon cluster with irregular patchy zoning near garnet grain boundary. P) CL image of zircon included in omphacite with indistinct patchy zoning.



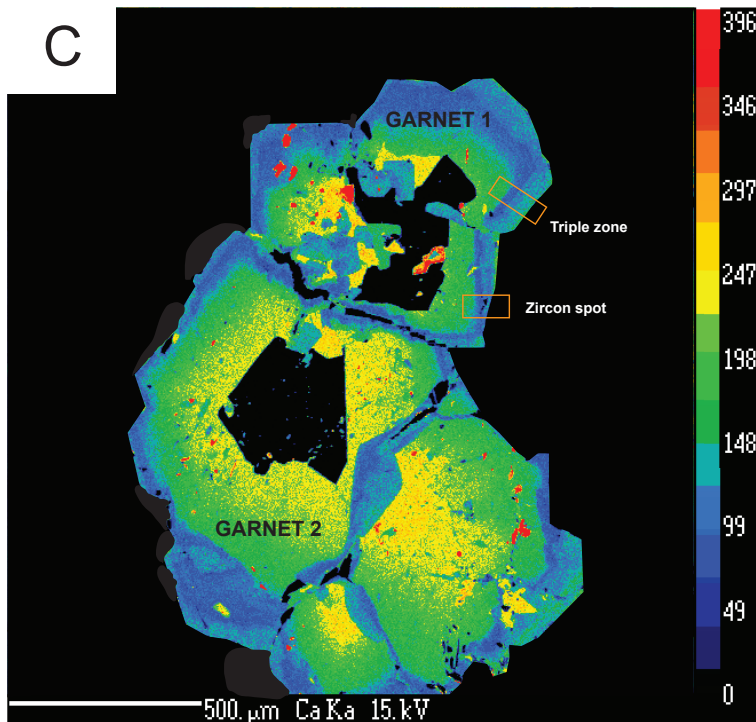
Supplementary Figure DR4 Age of Textural Settings.
 (A) Tera-Wasserburg Concordia plot of the U/Pb in CM71710-4 zircons included in UHP garnet; (B) garnet inclusions in omphacite; (C) CM71710-4 zircons in the matrix; (D) DD71710-2B zircons included in omphacite; (E) CM71710-4 zircons in the matrix; All analyses are uncorrected for common Pb. For each sample, lower and upper intercept ages of best-fit lines through all data are noted in the upper right.

Supplementary Figure DR4 continued. Age vs. Petrologic Setting. F) Petrologic settings of analysed zircons from DD71710-2b with ages > 45 Ma. UHP garnet = zircon included in UHP garnet; OI = zircon included in omphacite; MX = matrix zircon. G) Petrologic settings of analysed zircons from DD71710-2b with ages < 45 Ma. AMP = zircon included in amphibole. H) Petrologic settings of analysed zircons from CM71710-4 with ages < 45 Ma I) Petrologic settings of analysed zircons from CM71710-4 with ages > 45 Ma.

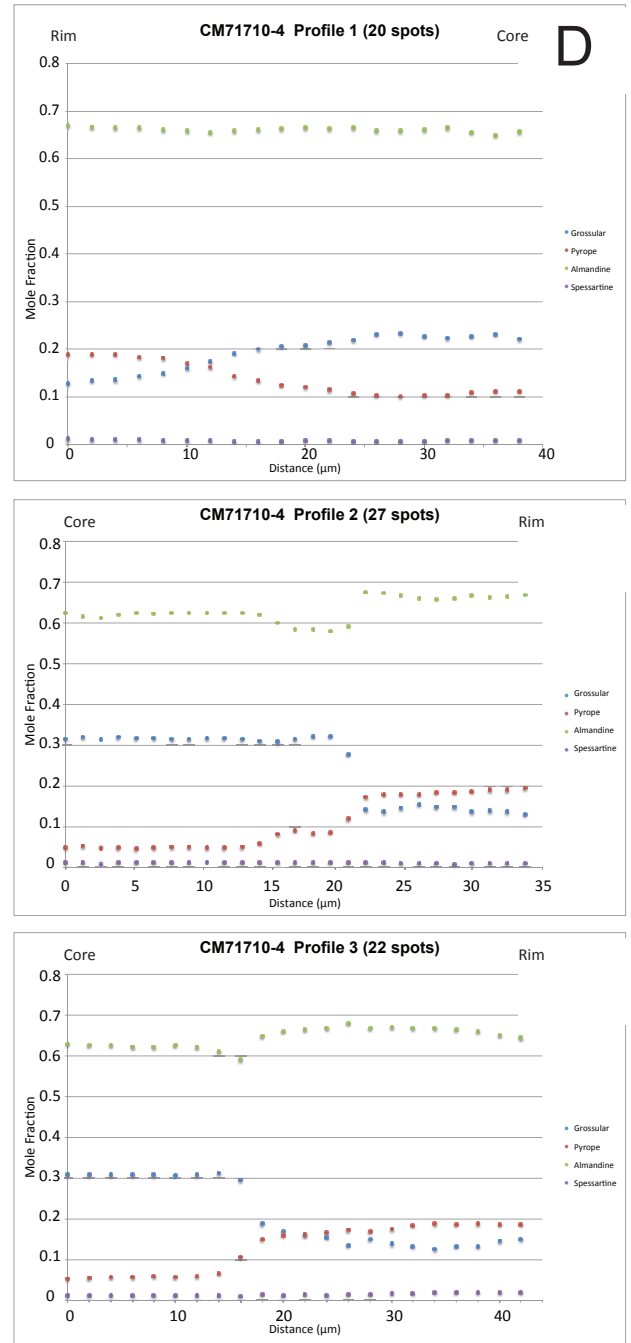




Supplementary Figure DR5



Supplementary Figure DR5. A. Color compositional X-ray maps of garnets in sample CM71710-4 reveal a strong zonation across a sharp boundary. The garnet composition is Ca-rich/Mg-poor on the core side of this boundary, while the rim side is Mg-rich/Ca-poor. B). Backscattered image of garnets from CM71710-4. The red square surrounds zircon analysis 9 (see Supplementary Table DR1), which yields 207 Pb-corrected U/Pb age of 44.4 ± 1.8 Ma. Profiles are marked in yellow. C) Masked Ca-X-ray map shown in A. Garnet I shows a distinct growth history with the calcium composition decreasing and subsequently increasing from core to rim. Zircon analysis 9 was taken in rim of the garnet with lowest calcium composition. In Garnet II, the sharp boundary signaling the strong difference in calcium composition is shown. D) Compositional zoning in these garnets is given with three profiles. Profile 1 shows a gradual increase in Ca composition and decrease in Mg composition from rim to core. Profile 2 shows a sharp decrease of Ca from core to rim. The Mg composition increases strongly coincidentally with the decrease of Ca composition. Profile 3 shows a similar pattern to Profile 2. Profiles 2 and 3 agree with data and observations from Tso Moriri garnet analyzed in Konrad-Schmolke et al., 2008.



Supplementary Table DR1. Summary of LA-ICPMS analysis of U-Pb isotopes in zircon from eclogite CM71710-4 and DD71710-2b in the Tso Moriri Gneiss Dome

Zircon	Analysis Spot	Texture	Elements (ppm)			Isotopic Ratios				Apparent Age					
			U	Th	Pb	$^{232}\text{Th}/^{238}\text{U}$	$^{235}\text{U}/^{206}\text{Pb}$	$\pm 2\sigma$ error	$^{207}\text{Pb}/^{206}\text{Pb}$	$\pm 2\sigma$ error	$^{206}\text{Pb}/^{238}\text{U}$ ^a	$\pm 2\sigma$ error	$^{207}\text{Pb}/^{235}\text{U}$	$\pm 2\sigma$ error	
CM71710-4	1	GR	46	2.0	1.8	0.043	117.8	7.29	0.240	0.020	41.2	2.1	250	24.0	
	2	OI	28	0.0	0.3	0.000	151	11.5	0.145	0.018	37.3	2.3	119	42.0	
	3	GR	79	0.4	0.5	0.005	126.4	7.0	0.081	0.007	48.6	1	86	69.0	
	4	MX	22	3.8	4.4	0.174	60	9.79	0.565	0.068	37.0	11.0	830.0	19.0	
	5	MX	32	0.0	3.9	0.000	70	5.02	0.407	0.029	49.9	4.2	595.0	87.0	
	6	MX	18	1.4	2.3	0.077	90.3	6.08	0.401	0.061	39.3	6	486	39.0	
	7	MX	12	1.4	2.0	0.122	97.1	9.37	0.383	0.074	38.1	6.9	439	19.0	
	8	MX	24	1.9	3.7	0.078	65.8	4.59	0.439	0.039	49.2	5.4	677	42.0	
	9	GR	25	0.2	0.4	0.008	128.4	7.91	0.136	0.014	44.4	1.8	134	39.0	
	10	OI	80	5.1	9.8	0.064	109	6.62	0.215	0.023	46.5	2	236	15.0	
	11	AMP	57	n/a	7.1	n/a	105	6.60	0.245	0.020	45.7	2.3	294	6.4	
	12	MX	94	8.9	19.8	0.095	107	7.17	0.339	0.033	38.0	3.0	372	15.0	
	13	OI	78	14.4	21.7	0.184	86.3	7.06	0.368	0.040	44.2	4.7	465	5	
	14	GR	47	1.0	7.0	0.021	87.2	8.50	0.283	0.028	51.7	5	378	42.0	
	15	OI	82	5.8	30.4	0.070	74.6	7.65	0.387	0.036	49.1	5.9	565	100.0	
	16	GR	35	n/a	0.5	n/a	119	9.16	0.137	0.028	47.8	3.4	140	34.0	
	17	OI	29	2.0	6.0	0.069	83.3	8.70	0.318	0.036	50.7	5.8	426	47.0	
	18	MX	63	18.4	14.0	0.293	89.3	9.84	0.385	0.041	41.2	5.5	488	11.0	
	19	GR	45	4.9	15.1	0.109	74.5	5.97	0.438	0.032	43.6	4.5	602	43.0	
	20	MX	54	6.2	8.2	0.114	94.1	7.43	0.264	0.030	49.5	4	330	33.0	
	21	OI	29	0.2	2.9	0.007	95.1	6.62	0.252	0.029	50.0	3.5	322	45.0	
	22	OI	62	8.0	9.2	0.129	99.5	8.13	0.272	0.031	46.2	3.9	325	71.0	
	23	MX	48	4.7	11.3	0.099	87.1	6.03	0.370	0.030	43.6	3.6	480	60.0	
	24	MX	144	2.3	4.1	0.016	124	7.23	0.123	0.013	46.7	2	131	54.0	
	25	OI	80	1.4	15.7	0.018	92.1	6.43	0.347	0.026	43.3	3.1	431	29.0	
	26	GR	27	1.1	19.6	0.041	45.2	5.22	0.606	0.048	41.6	9.8	1084	22.0	
	27	OI	76	26.3	7.7	0.346	104	6.54	0.223	0.020	47.8	2.4	265	21.0	
	28	GR	122	4.2	5.3	0.034	113	6.55	0.142	0.011	50.0	2	160	44.0	
	29	MX	115	1.4	1.2	0.012	134	7.52	0.096	0.008	45.0	1.2	94.5	19.0	
	30	OI	27	3.4	2.4	0.125	97.0	8.72	0.326	0.044	42.9	4.9	353	11.0	
	31	a	GR	34	1.1	7.2	0.032	82.6	7.24	0.390	0.031	44.0	4.4	506	49
	31	b	GR	32	0.9	0.4	0.028	119	9.31	0.197	0.033	43.6	3	206	22.0
	31	c	GR	49	3.8	15.7	0.078	69.9	5.69	0.379	0.031	53.3	5.0	566	39.0
	32	OI	170	0.6	2.9	0.004	147	9.79	0.118	0.021	39.8	2.1	105	91.0	
	33	GR	73	2.2	14.6	0.030	91.8	7.54	0.342	0.036	43.9	4.3	400	37.0	
	34	a	GR	89	3.4	8.4	0.038	109.1	11.7	0.278	0.040	41.7	5	330	34.0
	34	b	GR	40	n/a	0.5	n/a	124	8.32	0.163	0.021	44.2	2.4	166	38.0
	35	MX	57	n/a	53.6	n/a	44.8	3.29	0.579	0.036	46.9	7.3	1036	44.0	
	36	MX	49	3.4	12.6	0.069	96.0	7.04	0.385	0.043	38.3	4.2	453	73.0	
	37	OI	24	n/a	11.7	n/a	66.7	10.3	0.465	0.046	45.4	9	684	37.0	
	38	OI	91	n/a	33.4	n/a	78.2	5.84	0.403	0.028	45.2	3.9	535	49.0	
	39	GR	279	5.7	8.3	0.020	135	7.17	0.105	0.009	44.0	.9	104	53.0	
	40	OI	75	3.8	15.6	0.050	94.1	6.05	0.287	0.019	47.6	2.6	357	7.1	
	41	a	OI	116	1.9	28.6	0.016	91.5	5.39	0.317	0.020	46.2	2	400	20.0
	41	b	OI	46	n/a	7.0	n/a	96.1	6.85	0.294	0.029	46.0	3.4	367	21.0
	42	OI	36	2.1	10.1	0.059	85.9	5.30	0.408	0.029	40.7	3.2	516	36.0	
	43	OI	41	0.6	4.3	0.015	109	7.19	0.270	0.024	42.2	2.6	294	23.0	

Cont.

Table DRI Cont.

DD71710-2b	44	OI	74	4.8	3.2	0.065	112	7.54	0.246	0.022	42.2	2.5	269	27.0	
	45	MX	20	n/a	5.1	n/a	48	3.14	0.543	0.036	46.1	6.7	955	38.0	
	46	MX	22	0.4	8.5	0.018	38.5	2.62	0.633	0.036	38.1	8.5	1197	30.0	
	47	MX	51	3.0	8.5	0.059	62.1	4.75	0.496	0.030	42.2	4.9	765	48.0	
	48	MX	33	0.4	2.1	0.012	93.8	6.25	0.278	0.020	47.6	2.8	343	21.0	
	49	OI	25	1.5	1.6	0.060	98.4	5.67	0.287	0.021	44.6	2.3	345	16.0	
	50	OI	61	1.5	1.5	0.025	128.2	8.09	0.165	0.013	42.3	1.8	165	12.0	
	51	OI	151	7.2	0.3	0.048	148	8.12	0.054	0.005	42.9	1.0	50	4.0	
	52	OI	33	0.7	2.6	0.021	95.0	6.07	0.344	0.028	41.2	3.0	411	29.0	
	53	OI	30	0.1	2.4	0.003	94	6.53	0.354	0.028	40.6	3.2	415	22.0	
	54	OI	42	0.5	3.0	0.012	91	7.50	0.315	0.031	45.4	4.1	387	28.0	
	55	OI	27	0.6	4.7	0.022	61	4.5	0.478	0.035	45.4	5.5	725	48.0	
	56	GR	18	0.1	1.3	0.006	93	7.1	0.289	0.028	47.1	3.7	361	33.0	
	57	OI	40	n/a	2.6	n/a	103	7.12	0.302	0.030	41.3	3.2	344	29.0	
	58	MX	76	4.0	4.6	0.053	108.8	7.21	0.312	0.021	38.4	2.4	337	19.0	
	59	OI	29	0.5	2.5	0.017	77.8	5.49	0.324	0.028	52.4	4.1	476	38.0	
	60	MX	60	3.2	0.5	0.053	137.2	8.01	0.097	0.009	43.7	1.4	92	6.0	
	61	MX	38	2.2	4.1	0.057	81.2	6.25	0.432	0.038	39.0	4.6	558.0	42.0	
	62	MX	11	0.8	3.9	0.071	57.1	5.67	0.555	0.063	37.2	10.0	850	77.0	
	63	MX	42	0.8	0.3	0.019	128.4	8.10	0.092	0.010	47.1	1.9	96	10.0	
	64	MX	17	0.2	0.2	0.012	135.0	10.34	0.135	0.036	42.1	3.3	126	32.0	
	65	OI	78	7.3	5.2	0.094	121	7.46	0.127	0.014	47.6	2.0	137	15.0	
	66	OI	73	3.6	26.8	0.050	74.6	6.16	0.401	0.029	45.9	4.5	541	36.0	
	67	OI	58	6.5	31.4	0.112	62.2	3.83	0.467	0.028	46.2	4.3	708	26.0	
	68	MX	46	9.5	17.2	0.207	75.5	4.66	0.400	0.024	45.5	3.2	545	21.0	
	69	OI	36	0.7	4.5	0.020	96.0	7.74	0.225	0.023	51.2	3.8	287	27.0	
	70	OI	36	6.6	24.8	0.185	49.3	4.60	0.554	0.036	43.3	7	936	68.0	
	71	MX	119	3.1	18.7	0.026	103.8	7.18	0.271	0.022	43.6	2.8	311	27.0	
	72	OI	47	n/a	19.7	n/a	71.2	4.85	0.464	0.035	40.6	4.6	628	35.0	
	73	MX	34	n/a	8.1	n/a	85.3	5.99	0.331	0.027	47.1	3.6	414	27.0	
	74	MX	103	5.1	2.5	0.049	142	8.34	0.101	0.013	42.1	1.5	98.0	13.0	
	75	MX	54	17.2	16.2	0.321	84.6	5.49	0.326	0.023	48.0	3.1	425	24.0	
	76	OI	65	4.1	9.7	0.063	102	8.71	0.302	0.040	41.8	4.4	342	49.0	
	77	MX	52	0.6	39.7	0.012	50.8	3.62	0.522	0.031	47.3	5.8	898	36.0	
	78	MX	23	n/a	14.2	n/a	63.3	6.09	0.473	0.043	44.5	6.9	740	64.0	
	79	MX	125	18.4	76.3	0.148	59.1	4.44	0.482	0.031	46.4	5.2	764	48.0	
	80	OI	114	10.2	21.8	0.089	101	7.50	0.281	0.023	44.2	3.1	335	31.0	
	81	AMP	465	22.4	23.0	0.048	144	8.61	0.137	0.015	39.4	1.6	123	11.0	
	82	OI	145	8.7	33.2	0.060	88.5	9.00	0.310	0.033	47.4	5.3	400	57.0	
	83	OI	101	10.3	12.7	0.102	115	6.95	0.219	0.018	43.0	2.0	239	16.0	
	84	OI	34	2.6	27.7	0.077	51.8	3.93	0.552	0.036	41.5	6.5	917	44.0	
	85	OI	57	2.8	60.1	0.049	39.2	5.15	0.628	0.044	38.4	11	1180	110	
	86	OI	109	6.5	12.7	0.060	108	7.58	0.232	0.028	44.8	3.1	261	35.0	
	87	AMP	78	2.6	16.6	0.033	88.5	11.1	0.362	0.053	42.5	7.1	463	87.0	
	88	MX	129	5.7	24.1	0.044	97.2	5.99	0.279	0.020	45.9	2.4	342	22.0	
	89	OI	62	n/a	57.0	n/a	41.3	6.00	0.620	0.057	38.1	13	1110	150	
	90	OI	70	0.0	28.9	n/a	70.1	4.71	0.399	0.027	49.1	4.0	585	31.0	
	91	a	OI	49	3.7	15.6	0.075	79.7	5.60	0.362	0.028	47.2	3.8	478	33.0
	91	b	OI	118	7.1	15.7	0.060	99.1	8.48	0.263	0.031	46.4	4.2	324	45.0
	92	MX	35	5.4	18.7	0.156	62.1	5.26	0.482	0.035	44.1	5.7	723	54.0	
	93	MX	104	24.9	28.7	0.240	94.1	6.34	0.336	0.030	42.3	3.3	410	32.0	
	94	OI	23	2.8	0.6	0.122	126	13.8	0.193	0.041	41.0	4.8	166	30.0	
	95	OI	54	6.0	20.7	0.110	72.2	5.55	0.404	0.028	47.1	4.4	578	40.0	
	96	OI	72	1.2	75.2	0.017	42.0	3.52	0.596	0.037	42.3	8.3	1089	50.0	
	97	OI	55	6.1	20.7	0.112	74.5	4.92	0.394	0.026	46.8	3.7	550	28.0	
	98	MX	71	1.1	35.6	0.016	66.8	5.02	0.471	0.033	42.5	4.9	672	45.0	
	99	MX	77	4.6	16.8	0.060	103	6.54	0.326	0.025	39.5	2.6	366	20.0	
	100	OI	155	8.5	10.7	0.055	117	8.17	0.142	0.018	48.1	2.7	160	20.0	
	101	OI	40	0.1	38.9	0.002	44.2	4.16	0.579	0.040	43.4	9	1040	61.0	
	102	OI	101	15.0	6.3	0.149	129	7.78	0.163	0.019	42.1	1.9	160	16.0	
	103	OI	37	0.9	24.9	0.025	55.6	4.39	0.548	0.036	39.3	6.2	852	53.0	

Note: Both samples were analyzed 09/01/2011 and 02/17/2012, for which the error in standard deviation is (2 σ). Common Pb is corrected by projecting a line through all analyses to 207Pb/206Pb and 238U/206Pb on the Tera-Wasserburg Concordia diagram (Figure 2). a Age corrected for 207Pb. AMP (amphibole- zircon inclusion in amphibole grain), GR (zircon inclusion in UHP garnet), MX (zircon in the matrix near omphacite, rutile, titanite, amphibole other matrix minerals), OI (zircon inclusion in omphacite grains).

Supplementary Table DR2

Laser ablation single-collector inductively coupled plasma mass spectrometry analyses of rare earth elements in zircon.

Sample	Zircon	Analysis Spot	La	Ce	Pr	Nd	Sm	Eu	Gd	Tb	Dy	Ho	Er	Tm	Yb	Lu
10			0.173	5.87	0.77	1.72	2.2	3.6	94.2	100.7	146.2	173.4	275	335	551	776
11			n/a	0.43	0.21	0.80	1.2	2.5	48.4	41.8	38.4	36.2	43.2	38.1	58.6	65.0
12			0.007	2.50	0.44	0.37	10	46	68.5	36.7	32.4	24.9	42.8	53.6	98.5	159
13			0.030	1.11	0.20	1.30	6.5	14	51.1	40.5	38.6	30.2	24.0	35.2	53.7	71.4
14			0.147	5.81	1.42	2.97	5.5	13	20.1	19.6	23.3	21.2	29.0	26.8	48.0	54.9
15			0.214	7.35	2.85	7.39	4.2	4.2	62.2	50.3	47.4	41.8	47.7	69.2	75.4	95.8
16			0.029	0.58	0.57	n/a	8.6	23	56.7	52.7	86.2	91.2	121	134	154	156
17			0.054	0.58	0.45	0.35	6.4	20.4	33.6	40.7	46.2	59.4	79.2	76.8	83.6	101
18			0.050	0.95	0.63	0.35	7.0	17	20.8	33.2	27.9	26.8	37.4	41.4	51.5	76.2
19			0.041	0.69	0.19	0.46	10	18	27.3	30.4	54.1	82.6	111	130	211	247
20			0.009	3.59	0.41	1.04	17	22	84.4	135	237	374	710	1226	2394	2926
21			0.050	0.24	0.17	0.19	1.6	6.2	14.3	15.1	16.4	14.0	15.4	15.8	16.6	26.5
22			0.010	1.00	0.20	0.81	4.7	16	49.2	44.2	64.3	117.6	242	384	731	1099
23			0.014	0.61	0.22	1.01	9.4	26	37.6	41.6	34.6	41.5	47.9	70.8	65.6	78.3
24			0.038	1.40	n/a	0.61	13	42	75.5	66.9	64.8	68.1	70.7	67.0	80.4	61.9
25			n/a	1.49	0.41	0.74	4.1	24	42.9	27.3	34.7	29.8	34.5	33.8	38.0	34.5
26			0.031	0.35	0.38	0.42	4.9	12	20.0	22.3	24.4	31.4	33.4	34.7	38.9	49.1
27			0.059	0.82	0.35	0.84	4.1	13	22.1	18.4	11.6	19.2	30.9	46.9	81.9	130
28			0.003	0.60	0.36	0.62	6.9	16	31.1	47.9	70.1	116	229	300	379	428
29			0.043	1.40	0.77	0.90	19	57	82.3	75.7	62.0	64.3	97.7	134	173	171
30			0.021	1.61	0.35	0.73	10	24	40.5	43.7	37.3	37.3	49.8	42.6	48.3	50.3
31			0.039	0.58	0.19	0.56	6.4	27	51.6	48.6	60.7	69.8	92.2	92.0	108	117
31		a	0.061	2.12	0.32	n/a	4.1	14	25.3	28.9	39.8	49.8	60.1	58.6	61.9	74.7
31		b	0.025	0.33	0.12	0.39	4.5	21	46.9	52.5	37.6	34.1	28.4	37.0	30.3	37.3
32		c	0.031	0.22	0.14	0.47	4.1	12	20.1	19.5	18.4	17.7	24.1	24.8	28.3	36.2
33			n/a	1.43	0.65	0.90	13	53	92.9	68.6	54.1	45.0	54.4	50.2	47.3	51.9
34		a	0.049	0.43	0.17	0.69	5.7	16	34.6	27.4	29.3	32.1	32.1	17.6	30.4	53.7
34		b	0.003	0.98	0.27	1.04	16	35	63.6	59.2	43.8	45.6	61.1	76.6	172	240
35			n/a	0.75	0.08	0.60	6.9	24	43.3	54.2	70.8	89.3	107	110	158	173
36			0.003	1.00	0.18	0.50	5.0	20	42.0	40.0	56.2	65.3	82.9	67.8	68.1	67.8
37			n/a	0.39	0.37	0.29	4.8	13	20.0	24.7	20.6	13.3	25.4	22.6	24.2	30.9
38			0.030	0.34	0.12	0.01	.6	7.9	15.3	8.23	10.0	10.5	15.8	13.8	21.9	33.6
39			n/a	1.02	0.14	0.54	11	35	49.7	43.3	43.9	44.3	50.4	52.0	59.2	66.7
40			0.045	2.20	n/a	0.73	21	57	108	77.0	52.5	35.3	34.2	34.4	38.0	44.0
41		a	0.081	0.71	0.09	0.17	10	34	55.9	49.8	42.4	35.9	37.7	43.8	44.3	63.6
41		b	0.020	0.64	0.13	0.18	13	42	56.9	40.8	35.4	33.3	38.9	36.2	44.0	49.6
42			n/a	0.75	0.17	0.46	7.5	18	29.8	27.9	26.0	32.0	30.8	26.0	39.8	42.1
43			0.014	0.45	0.10	0.98	4.4	11	15.9	22.0	20.2	21.7	25.0	24.1	36.2	43.2

TABLE DR2 cont.

Sample	Analysis	La	Ce	Pr	Nd	Sm	Eu	Gd	Tb	Dy	Ho	Er	Tm	Yb	Lu
DD71710-2b															
65		0.004	0.225	0.075	0.216	7.40	16.7	22.3	35.1	33.3	38.4	37.6	43.4	39.9	49.4
66		n/a	1.277	0.766	1.728	7.25	18.7	28.7	45.0	32.5	36.2	38.7	53.9	35.9	61.1
67		0.011	1.164	n/a	0.320	5.92	17.5	18.6	29.8	24.5	28.1	29.1	37.1	35.2	43.3
68		0.037	0.685	0.315	1.176	9.70	21.6	29.5	43.7	36.1	42.8	40.5	55.1	38.3	121
69		0.021	0.833	0.159	n/a	7.52	11.5	26.5	34.6	33.5	36.3	37.1	40.5	61.0	61.0
70		0.247	17.654	2.800	6.766	9.68	13.1	18.8	49.5	43.3	56.1	59.5	100	127	177
71		0.051	1.748	0.145	0.867	9.43	30.2	43.9	56.3	38.1	41.1	34.9	37.5	33.6	60.2
72		0.013	1.067	n/a	0.811	7.30	38.4	51.5	46.4	31.4	37.4	27.1	33.5	29.4	50.4
73		0.016	0.813	0.112	0.316	11.0	39.6	51.7	59.6	54.5	47.8	47.2	36.6	48.9	62.0
74		0.040	1.551	0.234	0.614	11.4	47.1	67.8	81.5	65.2	42.8	47.5	48.9	65.9	65.9
75		0.029	1.394	0.211	0.924	6.30	15.8	27.6	36.8	43.1	60.7	89.6	118	232	232
76		0.047	0.466	0.186	0.492	2.45	8.65	25.6	29.3	26.7	25.6	22.2	32.9	28.5	41.9
77		0.027	0.698	0.180	0.331	3.63	6.59	11.0	20.3	19.8	18.8	21.9	19.8	17.6	36.6
78		0.025	0.421	0.226	n/a	4.27	15.0	36.1	43.3	32.7	32.7	31.7	39.0	33.5	45.9
79		0.050	3.687	0.734	1.705	14.8	48.3	80.2	112	106	170	175	242	333	450
80		0.033	2.613	0.637	2.446	10.7	36.9	46.9	63.5	54.9	70.1	61.5	83.4	78.7	100
81		0.025	2.629	0.144	0.422	9.92	44.5	88.6	101	82.6	88.5	73.3	73.5	91.0	91.0
82		0.006	1.603	0.105	n/a	5.62	32.2	54.3	60.2	43.5	41.4	46.5	49.6	59.8	59.8
83		0.004	2.412	n/a	0.263	14.5	62.9	73.4	80.5	58.4	58.3	53.2	51.2	42.2	83.2
84		n/a	0.235	0.310	0.673	4.81	4.81	23.7	26.7	21.9	25.2	29.4	30.4	33.5	46.2
85		n/a	0.941	0.106	0.433	6.40	10.3	24.8	28.6	30.1	33.4	27.3	26.4	33.3	42.5
86		n/a	0.835	0.135	0.386	5.44	25.2	38.4	52.2	55.9	61.3	75.0	85.6	90.2	144
87		0.090	1.841	0.262	2.169	8.24	21.2	37.6	37.3	30.4	22.7	29.6	33.9	21.3	77.8
88		0.009	1.987	0.205	0.544	8.91	8.91	34.2	50.7	53.9	56.2	68.4	80.9	116	209
89		n/a	1.066	0.343	n/a	1.55	1.55	29.4	39.6	28.4	27.3	32.9	54.9	54.4	62.3
90		0.060	0.548	0.223	0.626	4.07	18.0	29.8	40.9	38.5	31.2	38.2	37.5	47.5	54.9
91		0.014	1.405	0.337	0.837	7.88	26.3	38.0	38.9	27.2	22.3	28.2	41.4	41.1	61.2
92		0.058	1.390	n/a	0.319	4.82	35.2	39.4	42.9	35.9	21.6	30.7	57.8	44.8	61.1
93		0.024	0.154	0.277	0.357	1.05	6.75	14.3	18.1	12.2	16.6	24.2	21.3	40.6	53.3
94		0.049	1.469	0.472	0.857	6.88	15.4	24.0	26.1	32.2	37.6	54.3	54.8	116	147
95		0.041	0.160	0.150	0.305	3.04	45.9	68.3	76.9	69.2	50.6	59.9	50.8	56.5	61.2
96		0.037	0.507	0.172	0.350	2.35	9.58	22.2	25.1	25.6	23.6	26.9	40.3	48.5	48.5
97		0.000	0.317	0.259	0.460	2.05	2.07	23.5	27.9	17.4	22.2	23.8	36.1	32.4	44.5
98		0.027	1.262	0.337	0.625	3.86	25.5	32.9	36.8	31.1	35.2	41.4	45.3	60.1	93.9
99		0.060	1.330	0.419	0.753	4.22	38.4	30.5	46.4	26.9	37.4	27.1	24.6	25.4	27.2
100		0.033	0.970	0.445	0.709	7.61	21.9	22.6	34.8	26.7	22.1	27.2	24.5	26.0	45.7
101		0.034	1.385	0.127	0.318	6.40	35.8	53.1	66.9	59.0	54.6	51.2	46.2	48.4	57.3
102		0.023	0.094	0.094	0.364	6.50	17.8	30.8	39.6	31.7	37.7	39.9	35.7	41.8	84.0
103		0.039	1.471	0.304	0.837	4.37	23.4	32.9	41.0	43.7	51.7	76.8	106	125	153
104		0.018	0.489	0.187	0.571	6.01	39.0	54.9	62.6	61.3	69.6	73.7	66.9	69.1	94.4

Note: Both samples were analyzed in situ (09/01/2011 and 02/17/2012). Analyses that were tripped by the detector or showed anomalously high abundances were excluded from the data. Those analyses were assumed to have experienced analytical error or exceeded the detection limits set by standards calibration. Analyses recorded under detection level are denoted n/a.

Table DR3. Timing of Collision Calculation Table. The collision table uses a simplified equation modified from Leech et al., 2005 to predict timing of collision as a function of UHPM depth, age of UHPM, convergence rate and slap dip. It is an example of possible collision ages considering new realistic convergence rates and subduction geometries. 100 km is the assumed depth of UHPM. The convergence rates used are bracketed convergence rates using the fastest and slowest convergence rates between 52 Ma and 46 Ma from White and Lister (2012). The age of UHPM is the interpreted age reported in this study. The slab dip is the angle of the subducting plate with the horizontal. Values are first order approximations of 28° (Guillot et al., 2004), 35° medium value, and 41° (Leech et al., 2005). Slab dip is assumed to be constant for each value. The dip geometries from Leech et al., (2005) assumes the slab dip angle inscreases with depth; a realistic assumption that has a slab dip angle of 41° at UHP conditions. Initial subduction of the leading edge of the Indian Continental Margin ~51-47 Ma is under the assumption that UHP metamorphsim is a geologically brief event.

$$\text{Timing of Collision} = \frac{\text{Depth of UHPM}}{(\text{Convergence Rate} \times \text{Sin}(\text{Slap Dip}))} + \text{Age of UHPM}$$

Depth of UHPM	Convergence Rate	Slab Dip	Collision Age (UHP at 46 Ma)	Collision Age (UHP at 47 Ma)
100	69	28	49.1	50.1
100	69	35	48.5	49.5
100	69	41	48.2	49.2
100	150	28	47.4	48.4
100	150	35	47.2	48.2
100	150	41	47.0	48.0

White and Lister 2012: Convergence limits of 69mm/yr and 150mm/yr

Calculated collision ages provide minimum estimates for continental subduction timing, since the perserved UHP material may not represent the absolute leading edge of the subducting continent. The initiation of continental subduction corresponds to the timing of India-Asia collision under the assumption that the overriding plate was Asia (and not an island arc or microcontinent).

Supplementary References

- Corfu, F., Ravna, E.J.K., Kullerud, K., A Late Ordovician U-Pb age for the Tromsø Nappe eclogites, Uppermost Allochthon of the Scandinavian Caledonides. *Contrib. Mineral Petrol.* **145**, 502-513 (2003)
- Ludwig, K.R., User's Manual for Isoplot 3.00 a Geochronological Toolkit for Microsoft Excel (2003)
- Jackson, S. E., Pearson, N. J., Griffin, W. L., Belousova, E. A., The application of laser ablation-inductively coupled plasma-mass spectrometry to in situ U-Pb zircon geochronology. *Chemical Geology* **211**, 47-69 (2004).
- Paton, C., Woodhead, J. D., Hellstrom, J. C., Hergt, J. M., Greig, A., Mass, R., Improved laser ablation U-Pb zircon geochronology through robust downhole fractionation correction. *Geoch. Geoph. Geosy.* **11**, doi:10.1029/2009GC002618 (2010).
- Slama, J., Kosler, J., and Condon, D.J., Plesovice zircon—A new natural reference material for U-Pb and Hf isotopic microanalysis: *Chemical Geology*, v. 249, p, 1- 35 (2008)
- Wendt, I., Carl, C., The statistical distribution of the mean squared weighted deviation. *Chemical Geology. Isotope Science Section* **86**, 275–285 (1991).
- Wiedenbeck, M., Allé, P., Corfu, F., Griffin, W. L., Meier, M., Oberli, F., Von Quadt, A., Roddick, J. C., Spiegel, W., Three Natural Zircon Standards for U-Th-Pb, Lu-Hf, Trace Element and REE Analyses. *Geostandards Newsletter* **19**, 1-23 (1995).

